Trending and Analysis of Payload vs. All Low Earth Conjunction Data Messages below 1,000 km, from 2016 through 2021

Lieutenant Colonel Daniel Moomey
Air Force Institute of Technology, Wright-Patterson AFB, OH, daniel.moomey@afit.edu
Dr. Rachael Falcon
Headquarters Air Force Safety Center, Kirtland AFB, NM, rachael.falcon.ctr@us.af.mil
Arbab Khan
Booz-Allen-Hamilton, Lorton, VA, khan_arbab@bah.com

ABSTRACT

The Air Force Safety Center is developing a program to quantify the distribution of risks to the orbital environment across time and space by trending and analyzing orbital conjunction events. Previous efforts described automating the intake of Conjunction Data Messages (CDM) previously generated by the 18th Space Defense Squadron (18 SDS) and developing pre-processing scripts necessary to populate information germane to orbital collision risk assessment. The intent of the current effort is to account not only for the probability of collision (Pc), but also the consequence of the debris products from a collision to the low Earth orbital environment, should it occur. To accomplish this, CDMs of conjunction events below 1,000 km in altitude, between 1 Jan 2016 and 31 Dec 2021 were analyzed. 18 SDS reported Pcs were re-computed using the Foster-92 method. A circular 2-dimenaional interaction area was applied instead of a square, to reduce conservatism and lend closer towards realism. Hard Body Radii estimates were pooled from externally sourced information, including The Aerospace Corporation and various open sources. When not available, radius estimates were imputed based on available data. Covariance information was sourced from CDMs. For consequence, the amount of damaging, lethal non-trackable and trackable debris products were estimated using The Aerospace Corporation's IMPACT 8.0 model. The model accounts for relative velocity, object masses, distribution, and structure. Object distribution and structure were inferred from the object type field in the CDMs. Relative velocity was also sourced from CDMs. The object masses were sourced from data furnished by The Aerospace Corporation and Union of Concerned Scientists satellite database. The expected number of damaging, lethal-non-trackable, and trackable debris products were multiplied by the Pc to produce a quantitative risk metric for each conjunction event. Risks were adjusted to account for likely collision avoidance maneuvers based on satellite age, mass, and Pc. The results show a logarithmic increase in total risk over time, particularly after 2020. This change correlates to the arrival of Starlink and OneWeb satellites on orbit, and analysis confirmed that the uptick in risk is attributable to the arrival those large constellations on orbit. The risk metric for Starlink vs. Starlink conjunctions was further adjusted to more accurately account for proprietary processes and high accuracy ephemerides which enables better information for performing collision avoidance maneuvers. This adjustment reduced the slope of the risk trends starting in 2020, but they are still positive and logarithmic. Spatial domain analysis revealed that the preponderance of debris production risk for reported conjunctions below 1,000 km resides between the altitudes of 450 km and 850 km. The spatial distribution of risk by altitude changed starting in 2020 due to the arrival of large constellations at both their operational altitudes, and as a function of orbit raising operations, resulting in a higher and more evenly distributed risk of debris production above 350 km. Results also indicate that more trackable debris would have likely been generated by collisions between payloads and trackable objects, with perigees below 1,000 km than the 37 that have been confirmed and cataloged during that time period. However, analysis of the four confirmed payload collision events with cataloged debris produced a bootstrapped confidence interval of trackable debris generated per year suggesting the trackable debris production rate estimated here is within a plausible range. Planned future work looks to address known assumptions and limitations. This work is the first known effort to quantitatively analyze historical risks of conjunction events using full sets of CDM data and fuse them with the latest semi-analytical breakup algorithms. Analyses such as these are necessary to better inform ongoing and future Space Safety and Space Traffic Management policy development efforts within the US Government and internationally.

1. INTRODUCTION

Collisions between orbital objects pose a threat not only to operational satellites involved in collisions, but also to the broader orbital environment. Collision events have the potential to produce large quantities of debris, each of which then presents additional risk for further collisions. The quantity and size distribution of potential debris products has a large effect on the knock-on consequences to space operations and the sustainability of the environment thereafter.

The 18th Space Defense Squadron (18 SDS), located at Vandenberg Air Force Base, California, monitors objects in orbit and generates Conjunction Data Messages (CDM) with information about upcoming conjunctions – potential collisions – up to seven days prior to the Time of Closest Approach (TCA). Trending and analytics of conjunctions with a focus on the sustainability of the operational environment is currently outside the scope of the 18 SDS's mission, but it is part of the Headquarters Air Force Safety Center (HQ AFSEC) mission.

Air Force Instruction 91-202, *The US Air Force Mishap Prevention Program*, states that HQ AFSEC "…performs Air Force-level trend analysis of mishaps, incidents, risk, hazards and errors, and publishes results" [1]. Potential collisions, or conjunctions, between two Earth orbiting objects constitute a known quantifiable hazard to ongoing space missions and present a systemic and persistent hazard to the sustainability of space operations in the orbital environment. In 2018, AFSEC, Space Safety Division (AFSEC/SES) embarked on an effort to develop a hazard trending and analysis program using the CDMs produced by the 18 Space Control Squadron (now 18 SDS). AFSEC/SES published initial findings in 2020 [2]. That analysis identified low Earth orbit (LEO) environment as the highest risk orbit class, particularly below 1,000 km altitude.

The overarching goal of these analyses is to take the next step to analyze these risks in greater quantitative depth by assessing not only the probability of a collision, but also the consequence of the debris products from a collision, should it occur to the LEO environment. Multiplying the Probability of Collision (Pc) by the quantity of debris products of different sizes which are expected to be generated if a collision were to occur produces a risk metric interpretable as the expected risk of debris generation for the event. That risk metric is then analyzed both spatially and temporally for the LEO regime below 1,000 km where the risk was previously analyzed to be the highest of all orbital regimes [2]. The intent of performing these analyses is primarily to provide useful information for space safety policy development such as orbital debris mitigation, remediation, and regulatory rule making for commercial space launch and operations at all levels of government HQ AFSEC is involved with.

This is somewhat of a different approach than the typical application of the 18 SDS CDM data, which are primarily used to inform acute Conjunction Assessment (CA) risks. Operational perspectives on the risk posed by a collision tend to focus on the Pc since any hyper velocity collision between an object large enough to be cataloged and a satellite vehicle can be assumed to be a mission ending event [3]. The decision to execute a Collision Avoidance Maneuver (COLA) is primarily based on a cost to benefit analysis as it pertains to the mission of the vehicle of reducing the Pc below a determined threshold (usually to the order of <1e-6) [4]. However, from the perspective of attempting to assess and trend the risk of debris generation and its knock-on effects to the future environment sustainability, more nuances should be applied to the consequence component of the risk calculation. To do so across a cross section of all historical events below 1,000 km, such a broad brush requires applying assumptions and limitations to the data, which are outlined in the next section.

2. ASSUMPTIONS AND LIMITATIONS

The data spanned the satellite catalog (SATCAT) of over 24,000 active objects, comprising of over 170 million CDMs, which sampled nearly 3 million individual conjunction events between 1 Jan 2016 and 31 Dec 2021. Processing such a large data set requires employment of several processes, limitations, and assumptions, largely employed to quantify and reduce bias from the data with the aim of achieving zero-bias risk metrics. Work on further refining these assumptions and improving them continues, with the goal of more tightly bounding the confidence and rate of change of the problem of orbital debris.

(a.) Assume that the Central Limit Theorem dictates that with no bias, summing the Pcs over a set of conjunction events should see the difference between the sums of the Bayesian and the frequentist approaches converge towards zero as the number of events goes towards infinity [5,6]. The occurrence of

orbital collisions aligns inherently with the frequentist statistical perspective, i.e. a collision either happens or it doesn't. Though, without a priori knowledge of the outcome, industry standard approaches rely on statistical inference to calculate a Pc relying on fundamentally Bayesian approaches. The low number of confirmed collision events in the environment coupled with large uncertainty in attributing breakup events to small Radar Cross-Section RCS debris collisions vs. internal component or other failure modes makes it difficult to discern how well reality matches this expectation. Therefore, maintaining a Bayesian approach to this fundamentally frequentist problem is justified in this work by the fact that a significant number of events (several hundred thousand) are analyzed to calculate environmental risk. To accomplish this, several assumptions must be made regarding the data and the methods used to calculate individual event Pcs and consequences, which are discussed in the next section.

(b.) Assume that the 18 SDS satellite catalog (SATCAT) is complete down to an object size of 10 cm or larger.

(c.) Assume distribution of secondary objects represents the environment but acknowledge that limiting primary objects to be payloads only risks under sampling regions where the risk of orbital conjunctions involving only non-payloads is highest, such as Rocket Body vs. Rocket Body, Rocket Body vs. Debris, or Debris vs. Debris.

(d.) Limitation that the list of events occurring on orbit is incomplete. This list only includes Payload vs. All cataloged objects, i.e. the observable risk contribution of payloads to the debris environment. As of Sept 2020, 18 SDS has begun screening for non-payload conjunction events which reach emergency reportable criteria. A follow-on study is planned which will include an evaluation of All vs. All reported conjunction events, from 2021 through 2022.

(e.) Limitation that calculated risk may be somewhat sensitive to screening changes in CDMs by the 18 SDS. Though this is somewhat compensated by the normalization from multiplying consequence metrics by computed Pc. i.e. high Pc events which carry high risk can expect to be reported. Thus, the subset of events which fall outside of screening criteria, except for large derelict objects can reasonably be expected to be small.

(f.) Limitation that all collisions are assumed to fully overlap the primary and secondary objects, causing higher mass interaction ratios than would be expected. This limitation will be further evaluated and addressed by offsetting the mass interaction based on the ratio of the hard body radiuses (HBRs) of the interacting objects such that large ratios assume complete overlap and small ratios assume a 50% overlap. The magnitude of the inflation is hypothesized to be on the order of a factor of two or higher, but is expected to be less than an order of magnitude.

(g.) Limitation that object sizes are often inflated. Radius values are usually published as largest dimension or at best, a set of (L) x (W) x (H) dimensions, not average dimensions. When possible, average HBRs were computed and used. However, most of the objects in the catalog have a single source and value for physical dimension (which is presumed to be the largest dimension). Using the largest dimension of a vehicle to determine the HBR inflates the Pc by varying amounts, based on the ratio of the largest to smallest dimension for the shape of the objects considered.

Because an object may be struck from any direction relative to the body frame, if sampled numerous times, the interaction area can be approximated as a circle having a radius between r_{min} and r_{max} where r_{min} is the minimum linear radial dimension, and r_{max} is the maximum linear radial dimension. This can be further simplified as a circle with radius r_{mid}, where $r_{mid}= (r_{min} + (r_{max}-r_{min})/2)$. The aspect ratio of the largest to smallest dimension of space objects such as large GEO comm satellites and rocket bodies is generally a factor of 5 or less, leading to an assumption that the average aspect ratio of the catalog on average is lower than 5 and is hypothesized to be between 1 and 3 for most objects. Thus, if two objects are of equal size with an aspect ratio of 2, then the resultant Pc values may be an significantly lower, assuming an average aspect ratio than would otherwise be predicted. This might be indicative of a payload vs. payload conjunction. Whereas if the secondary object is a piece of small debris, the Pc would be inflated by less than a factor of two. When considering that large on large events carry the largest risk to the environment in terms of probabilistic debris production, this should be accounted for. Efforts are underway to identify

sources for multi-axis measurements and/or average HBR values for objects in the catalog and better account for the upward bias to Pc as a result.

(h.) Assume that multiple CDMs refer to the same conjunction if it is between the same two objects and the TCAs are within 22 minutes of each other. The 22-minute window accounts for potential changes to the TCA prediction, while also allowing for two objects to conjunct twice within the same revolution on opposite sides of the Earth. Using a 22-minute screening gate allows for the TCA to change by up to a quarter revolution in either direction.

(i.) Assume that each conjunction event is best represented by the latest CDM prior to the TCA.

The object state vectors and covariances are likely to be more accurate at TCA with a shorter propagation time [7]. Though if one of the objects maneuvered, or is sparsely tracked, this assumption may break down.

(j.) Assume that events with a Pc < 1e-10 were inconsequential.

(k.) Assume that CDMs where the 18 SDS computed Pc was not populated met one or more of the filtering criteria outlined in the spaceflight safety handbook for low relative velocity, covariance too small, covariance too large, etc. such that results from the Foster-92 algorithm might be unreliable [8]. This assumption was supported by a review of the relative velocities, covariances, and re-computed Pcs for a set of such CDMs. Several of the recomputed Pcs were unrealistically high, particularly in cases where one object's covariance was very small and the other was very large.

(l.) Assume payload objects are maneuverable if they have an International Designator less than 10 years from TCA and had an estimated mass greater than 100 kg. This is coupled to the assumptions that the mission lifetime of LEO satellites is typically ten years or less, and that smaller vehicles have a lower likelihood of being maneuverable. The applicability of this assumption does not address each individual event but is expected to apply well to the data set as a whole.

3. METHOD

The 18 SDS maintains a High Accuracy Catalog (HAC) of Earth orbiting objects which facilitates collision avoidance (CA) screening and warning services through Space Domain Awareness (SDA) sharing agreements using CDMs and operator requested screening [9]. The thresholds for screening and data contents of CDMs are governed by the 18 SDS' *Spaceflight Safety Handbook for Satellite Operators* [8] and the CDM Bluebook [10]. There are over 300 fields in each CDM. SDA information produced by 18 SDS, including CDMs, is shared with the space community via the public-facing website www.space-track.org [11]. Access to these data is provided via an Orbital Data Request (ODR) which is staffed through the 18 SDS and adjudicated by US Space Command (USSPACECOM) staff. After the ODR necessary to accomplish this work was submitted to the 18 SDS and approved, Space-track.org staff provided .csv files with all CDMs generated from 2016 through April 2020 to HQ AFSEC, which the AFSEC and the Air Force Institute of Technology (AFIT) research team members acknowledge and appreciate.

3.1. Data ingestion

Starting in May 2020, the research team accessed the data each day from the space-track Application programming Interface (API). Due to occasional technical glitches over the subsequent 20 months, several days of data were either missing or only partially downloaded. The missing data is of low concern for the present analysis because (1) the timing of the glitches was not correlated with orbital events so no bias was introduced, (2) the percentage of the data that were missing is extremely low, and (3) messages for an event are often generated over several days so the number of events that were missing is likely much lower than the number of missed days might suggest. This is being corrected for future studies by an agreement with space-track.org to integrate the message processing, data reduction, and analysis scripts within the space-track.org environment. The method herein closely reflects [12]. Though, the recent pivot to incorporate processes with space-track.org directly has forced modifications to the architecture and processes still under development. Additionally, this capability is being developed with the intent of allowing external user access to these data to members of the US Space Force (USSF) University Partnership

Program (UPP). A subsequent ODR has recently been approved to share these data with the USSF UPP. Efforts to architect and develop this capability are also currently underway.

3.2. Filtering by source of information

The initial data set consisted of 177,191,538 CDMs. Messages with duplicate CDM ID numbers were excluded. Messages based, at least in part, on ephemeris data provided by satellite Owner/Operator (O/O) were also excluded because (1) such messages are likely to bias the data by over representing active satellites, (2) such messages may represent proposed maneuvers which may or may not have occurred, and (3) the covariances and other values essential for subsequent analysis were often missing from these messages. Retaining only messages based entirely on the SSN's observations reduced the total data to 30,313,539 messages.

3.3. Identification of conjunction events

The 18 SDS performs initial screening seven days prior to TCA. Conjunction events are regularly re-screened, generating several updated CDMs prior to TCA. CDMs need to be matched to unique events which have the same primary object, secondary object, and TCAs close together in time. Based on assumption (h.) above, to match CDMs to conjunction events, the research team sorted the data by the ID number of the primary object, the ID number of the secondary object, and the TCA. A script then iterated over the sorted CDMs. If a CDM has the same primary object, and secondary object as the prior CDM, and it has a TCA within 22 minutes of the prior CDM's TCA, then it is assigned to the same event as the CDM above it based on assumption (h.) above. This process grouped the 30,313,539 messages into 2,906,984 unique events. Based on assumption (i.) above, the last CDM generated prior to TCA was retained for each event.

3.4. Filtering by altitude

To focus the analysis on the region of the orbital environment below 1000 km above the Earth's surface, we calculated an altitude for each conjunction event using the projected X, Y, Z coordinates of *primary object* at TCA and subtracting the mean Earth radius of 6,371 km. After filtering out events at an altitude above 1,000 km, 2,888,618 event messages remained.

3.5. Filtering by date

CDMs were selected based on the date that they became available through the space-track API. However, because CDMs are created in advance of TCA, and are made available through the space-track API after they are created, the remaining 2,887,832 CDMs included 2,167 with TCA in 2015 and 23,150 with TCA in 2022. Additionally, the data were parsed by week, which were partial in the first week of 2016 and last week of 2021. Therefore, analysis was limited to events with TCAs falling within whole weeks, ranging from 15 Jan 2016 through 23 Dec 2021. Friday was the cutoff day for each week because 1 Jan 2016 fell on a Friday.

3.6. Assigning radius and mass

Radius is needed to calculate collision probability. CDMs contain an Exclusion Volume radius, used by 18 SDS to calculate Pc, but most are default values for the object type, and do not correlate well to other publicly available sources of space vehicle dimensions. CDMs also contain an RCS, and [2] used an estimate based on these, but these values are highly susceptible to the object shape, orientation, and material, which cause poor correlation with known object sizes in general, though the National Aeronautics and Space Administration (NASA) has developed a Size Estimation Model (SEM) using the Haystack radar through the Orbital Debris Program Office [13]. Others have confirmed that
RCS can be used to estimate a rough estimate of the characteristic length of an orbital debris object [14]. In addition to object dimensions, object mass was necessary to estimate the amount of debris expected to be produced by a collision. Mass estimates were available from the Union of Concerned Scientists (UCS) for most active satellites, and from various other open sources for most rocket body objects in the catalog [15, 16]. A separate, accurate, external source was necessary for a few remaining objects, as well as for fragmentation debris objects. The Aerospace Corporation maintains estimates for object sizes and masses, including debris objects, which they made available for this research effort.

Mass was populated first from the UCS database when available, then from a list of rocket body masses compiled from public sources, then from the tables provided by The Aerospace Corporation. The UCS database has columns for both the Mass at Launch and the Dry Mass of a satellite. Launch mass was used where it was the only mass populated. Where both masses were populated, the mass at TCA was inferred by estimating the fuel usage rate from

the launch date and the expected lifetime of the satellite. This assumes the satellite vehicle would use all its fuel over the course of its expected lifetime, leaving only the dry mass thereafter, as computed from the following two formulas:

$$estimated\ fuel\ use\ rate = \ln\frac{dry\ mass}{launch\ mass} \Big/ expected\ lifetime\ (days) \quad \text{(eq. 1)}$$

$$mass\ at\ TCA = max\begin{cases} launch\ mass * e^{rate * age\ at\ TCA\ (days)} \\ dry\ mass \end{cases} \quad \text{(eq. 2)}$$

When a CDM object mass or radius could not be found in one of the available sources, these values were imputed. Imputations were based on the mass and radius values that were available from external sources as well as aspects of the objects in the CDMs, such as the object name, type, and RCS. Object types were missing from many CDMs and listed as Unknown or TBD for others. SciKit-Learn, IterativeImputer, and ExtraTreesRegressor Python tools and libraries handled the imputation from available data sources [17]. From among nearly three million conjunction events, which occurred between 2016 and 2021, the number and percent of the mass and size values which required imputation are shown in Table 1:

Table 1. Number and percent of events where mass and radius values were imputed

		Imputed	
		N	%
Primary Object	Mass	78,258	2.7
	Radius	136,261	4.8
Secondary Object	Mass	847,538	29.6
	Radius	404,664	14.1

The percentages of secondary mass and radius values imputed were high because debris objects are more difficult to ascertain and thus are disproportionately less represented in the data. However, the results section will show this likely has a low consequence to both the distribution of risk and it's total.

3.7. Re-computing Pc

The CDMs include a field for the Probability of a collision (Pc) between the two objects, produced by the 18 SDS using the 2-dimensional Foster-92 method [8]. However, 18 SDS commonly uses default radius values based on object type. Also, the 18 SDS integrates over a square area, rather than the circular area, leading to an inflated Pc. Therefore, Pc was re-computed to reduce known conservative bias in the results.

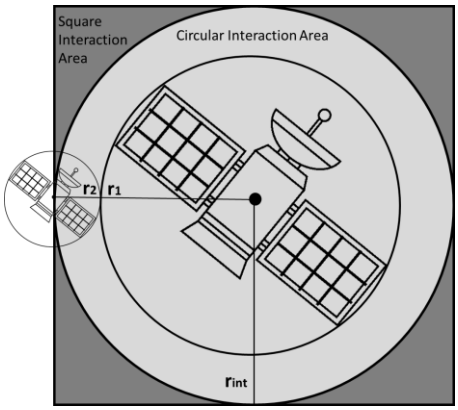

Fig. 1. Circular vs. Square Hard Body Radius (HBR) interaction area

NASA has developed a Conjunction Analysis Risk Assessment (CARA) MATLAB script for computing Pc with the Foster (1992) method [18]. The script was converted from MATLAB to python, and applied to each CDM in the database, using a circular interaction area and the improved radius values, which produced 434 Pc values > 1. The computed Pc was replaced with the 18 SDS Pc in the 228 CDMs where 18 SDS provided a Pc within the range 0 to 1 (inclusive). The remaining 206 CDMs with a computed Pc > 1 were excluded. The converted script was unable to

compute a value for 508 CDMs. None of these 508 incalculable cases had a usable (between 0 and 1 inclusive) 18 SDS provided Pc. The 508 incalculable cases were necessarily excluded.

Based on assumption (j.), events with a Pc<1e-10 were excluded to reduce processing time. Although approximately 2.2 million of the 2.8 million sampled events fell below this threshold, excluding these events resulted in the equivalent of excluding a single event with a Pc on the order of only 1e-8, which validated assumption (j.). Based on assumption (k.) the recomputed Pc was assumed to be unreliable for events that did not have a Pc provided by the 18 SDS, which totaled a little over 90,000 of the remaining 597,000 events, or approximately 15% of the remaining events. These events were also excluded. Lastly, there were an additional 95 events which 18 SDS recomputed Pc more than 1,000 times higher than the 18 SDS Pc. The results of these outlying events were also considered unreliable and were therefore excluded, leaving 503,247 individual conjunction events for risk evaluation.

3.8. Computing collision consequences

The IMPACT 8.0 algorithm was leveraged to calculate the consequence of each collision, should it occur. IMPACT was developed by The Aerospace Corporation, as part of the ADEPT suite [3]. The development of this semi-empirical model is the culmination of decades of work funded by NASA as well as by USSF Space Systems Command. The model has been informed by NASA, academic, and The Aerospace Corporation studies of historical breakup events, as well as by empirical collision lab tests such as the DebriSat and DebrisLV [19-21]. The IMPACT 8.0 algorithm was used to calculate the number of debris pieces for a set of over 500,000 collision conditions. The results generated predictions of the quantity and velocity distributions of debris products, ranging from 1mm to 1m+ in size. These data were organized structured as a set of look-up tables. These look-up tables accounted for the masses of each object, the overall structure of each object, and the collision velocity for each historical conjunction event. The velocity information was not leveraged for this work, though it could be incorporated to future research efforts to determine orbital lifetimes of the debris products and better inform the dynamic temporal nature of the risk to space operations. The collision cases were linearly divided into 90 bins, while the mass bins were separated logarithmically and covered 30 hollow body mass bins, 70 solid higher mass bins, and 80 solid lower mass bins (includes smaller debris). The results of the constituent debris were recorded across seven different size thresholds (1-3, 3-5, 5-10, 10-50, 50-100, 100-1000, and 1000+ mm in size). These results were further binned into damaging (1-10 mm), mission lethal but not trackable (LNT) (1-10 cm), and trackable (10 cm +) debris. Figures 2 and 3 below show how the results from the IMPACT algorithm vary based on collision input parameters. There is a state transition indicated by the diagonal blue line. Collisions falling above the transition are considered catastrophic which is dependent on the specific collision energy of the event. The heat map indicates the number of pieces of debris above a threshold of ≥1cm in size for each of the collision conditions indicated on the axes. Four of these were generated, for solid vs. solid, solid vs. hollow, hollow vs. solid, and hollow vs. hollow, whereby the first object is the higher mass object involved in the modeled collision.

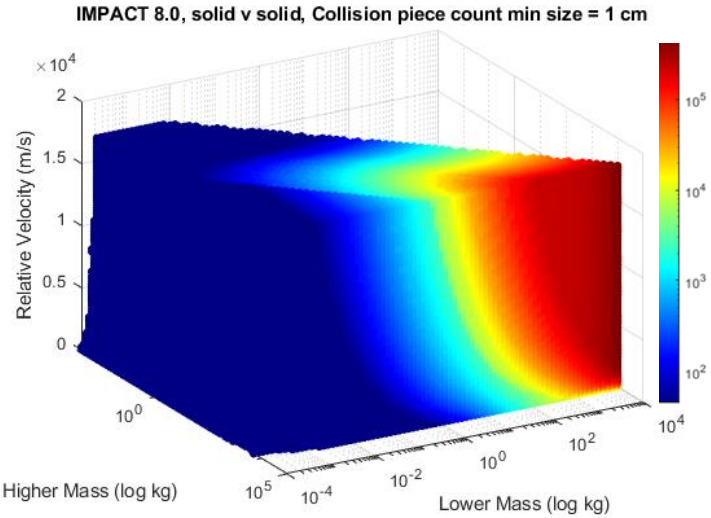

Fig. 2. Heatmap of number of debris products larger than 1 cm for Solid vs. Solid object collision cases

The following example provides a reference for the distribution of the number of debris pieces generated for two solid space objects colliding at 14 km/s.

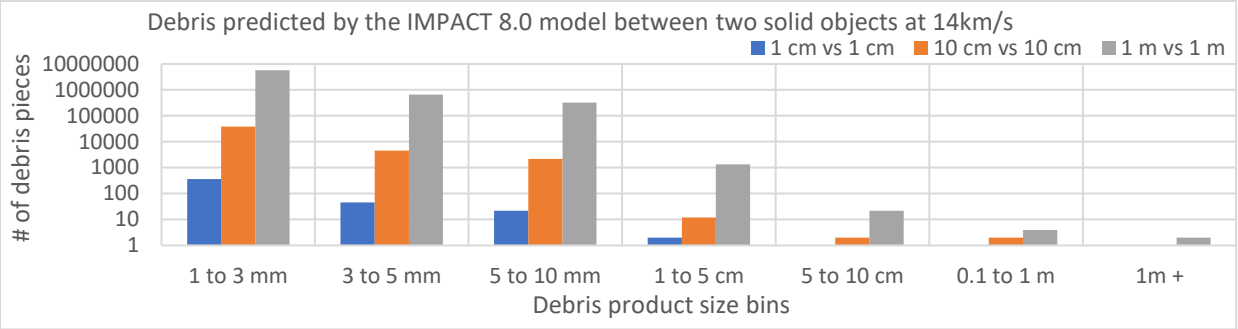

Fig. 3. Example logarithmic distribution of debris for solid vs. solid collisions of different sized objects at 14km/s

3.9. Risk metric

With the probability and consequence calculated for each conjunction event, the risk (*R*) of each event (*n*) was computed as the product of the number of damaging (*DMG*) / lethal, non-trackable (*LNT*)/ and trackable (*TRK*) debris pieces which would be produced, and the re-computed Pc (Pc_r) and mitigation factor (*MF*), where the region of 1 to *n* is a subset of events of interest for analysis.

$$R\_DMG_n = \int_1^n Debris\_DMG_n * Pc_{rn} * MF_n \quad \text{(eq. 3)}$$

$$R\_LNT_n = \int_1^n Debris\_LNT_n * Pc_{rn} * MF_n \quad \text{(eq. 4)}$$

$$R\_TRK_n = \int_1^n Debris\_TRK_n * Pc_{rn} * MF_n \quad \text{(eq. 5)}$$

3.10. Accounting for COLA maneuvers

While reviewing the initial risk results, and as was expected, it became clear that maneuvers need to be accounted for. Unfortunately, there is no publicly available database which contains the information on what maneuvers are executed, when, and for what reasons. So, additional assumptions became necessary. Absent a list of operational and maneuverable vehicles for each week, spanning the six-year period, for the purposes of this analysis, objects labeled as "PAYLOAD", whether they were the primary or secondary object were assumed to be maneuverable in accordance with assumption (l.). This of course is not 100 percent accurate for each specific case but is a reasonable assumption when considering summary risk metrics of a large set of events. Additionally, due to the maneuvering strategies implemented by Starlink and OneWeb, if either satellite in an event included Starlink and the recomputed Pc was ≥ 1e-5, the event was assumed to be mitigated to 1e-6. If either satellite included OneWeb and the recomputed Pc was ≥ 2e-5 or the miss distance was < 100 m, the event was assumed to be mitigated to 1e-6 [22-24]. Lastly, additional considerations for Starlink vs. Starlink conjunction events were necessary.

3.11. Accounting for large constellation self vs. self conjunction events

The large LEO communications constellations had a higher proportion of total weekly risk than was expected. Figure 4 a-c illustrate the Iridium (Fig. 4.a), Starlink (Fig. 4.b.), and OneWeb (Fig. 4.c.) constellations' proportion of the total risk for each week. Prior to 2020, Iridium's median proportion of risk was about 10%. Both Iridium's peak and median proportions dropped dramatically after Starlink and OneWeb began to launch. However, this was not due to a reduction in Iridium's total risk per week, but due to an uplift in the total weekly risk in general. During 2020 and beyond, risk proportions for Starlink and OneWeb have each risen to constitute a significant portion of the risk. Note that a higher interaction rate between Starlink and OneWeb has emerged, such that in later weeks, summing the risk proportion involving Starlink and the risk proportion involving OneWeb may exceed 1, indicating interactions between large constellations passing through each other may begin to dominate the risk picture, which should be monitored.

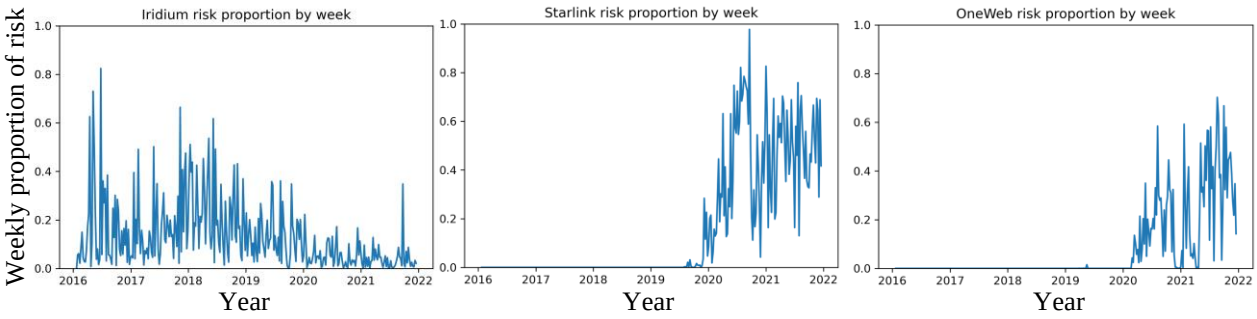

Figs. 4a-c. Proportion of total risk involving the Iridium, Starlink, and OneWeb constellations, respectively

Considering the regularity of relatively close spacing and common altitudes that these constellations operate in, it was worth exploring the question of how much of these risks originated from self vs. self conjunctions. O/Os typically maintain high accuracy ephemerides for each of their vehicles. This is certainly true for the three constellations identified above, which utilize their proprietary flight safety processes. It should also be noted that 18 SDS does not consider vehicle ephemerides in its Pc calculations for CDMs when relying on its own orbit estimations from the Space Surveillance Network. While the 18 SDS provides ephemerides screening as a service, it is not clear from amongst those data, which are real vectors and which are possible planned maneuver vector screening requests and thus they were not included in this analysis. Thus, the true risk vs. the calculated risk in the data likely does not scale properly using the Foster-92 algorithms and the state vectors and covariance values determined by 18 SDS. So a Risk Reduction Factor (RRF) should be considered in an attempt to account for this disparity. Without Starlink ephemerides, estimates for this differential were inferred from publicly available information, shown in Figure 5 [25].

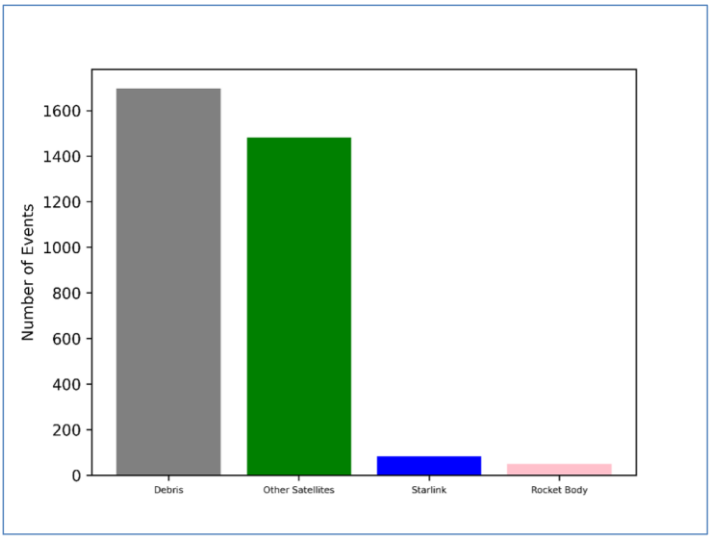

Fig. 5. Number of Starlink maneuvers from July-Dec 2021 [25]

The estimated total number of maneuvers from this chart is 3,319 ± 16, with 85 ± 4 being Starlink vs. Starlink. This ratio was then compared to that of the CDMs over the same period. All Starlink events with a re-computed Pc >1e-5 accounted for 43,042 events. 35,047 of those were Starlink vs. Starlink. Taking the ratio of the ratios of Starlink vs. All and Starlink vs. Starlink for the actual maneuvers conducted vs. those predicted by the Foster-92 algorithm which meet the Starlink maneuver criteria of >1e-5 yields that Starlink maneuvers about 169 times less often than would otherwise be expected (shown in Table 2).

Table 2. Calculated RRF based on proportions of Starlink maneuvers to reported events by secondary object type

Events > 1e-5 from Jul-Dec 21				
Source	SL vs. SL Maneuvers	SL vs. Other Maneuvers	Ratio	Risk Reduction Factor
CDMs	35,047	7,995	4.387	157 to 175
Starlink	85 ± 4	3,234 ± 12	0.026 ± .001	

A Risk Reduction Factor of 169 was calculated and applied to each Starlink vs. Starlink event, meaning the risk of debris production for these events was mitigated a further 169 times. It is assumed the reduction of actual maneuvers to expected maneuvers is largely due to high accuracy ephemerides which are shared between Starlink vehicles, and Starlink's use of a proprietary 3-dimensional Pc calculator which combine to yield higher fidelity awareness for both the primary and secondary vehicles than is known strictly from observations collected by the Space Surveillance Network.

When high accuracy ephemerides are not known for Starlink vs. Other events, it is assumed that Starlink utilized the 18 SDS Pc values to determine whether an event met the >1e-5 threshold for maneuver. Additionally, Starlink advertises a capability to perform a "ducking" action, which may further mitigate low probability events where maneuvers are not expected. However, the ducking action was not modeled for these results. After accounting for the Starlink vs. Starlink risk reduction factor, Starlink's share of the total collision risk per week dropped by about a factor of two to four, as shown below in Figure 6.

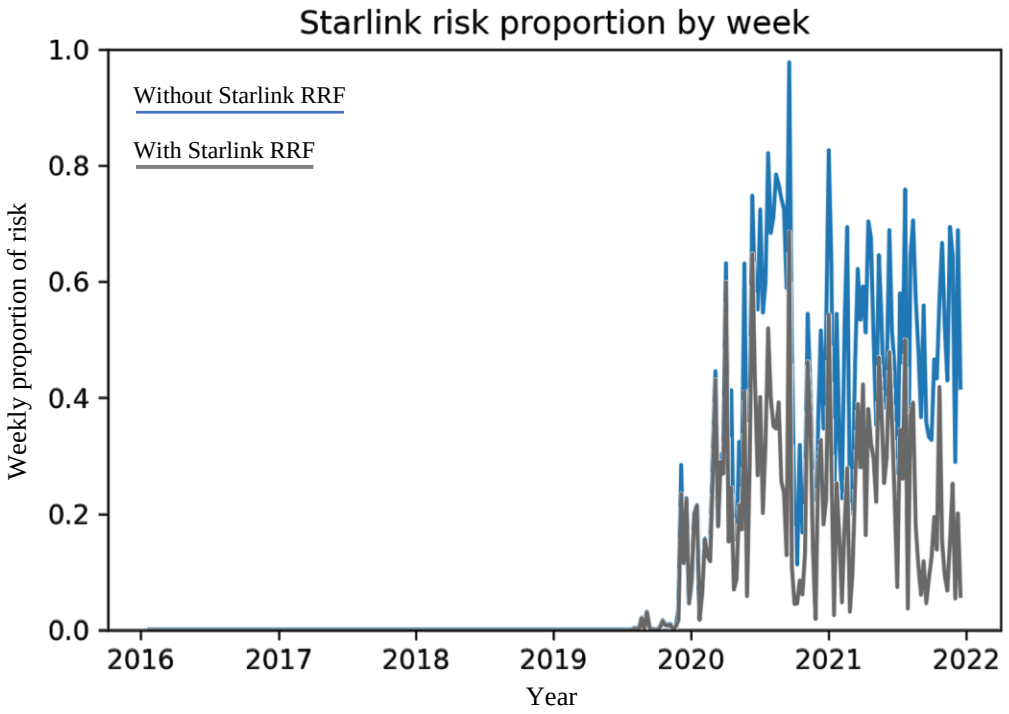

Fig. 6. Starlink vs. Starlink risk with and without considering Risk Reduction Factor

These results indicates that the application of high accuracy ephemeris for CA purposes is substantial in reducing the overall risk. Aside from Starlink, OneWeb vs. OneWeb and Iridium vs. Iridium did not yield significant contributions to the overall risk to warrant similar RRF analyses. The Starlink RRF was applied to all results shown in the analysis section below.

4. ANALYSIS

4.1. Temporal risk analysis

The risk metric for all events was summed over weeks. Figure 7 shows the results for the number of trackable, LNT, and likely vehicle damaging/mission degrading debris products expected to be produced for each week from 2016 through 2021. Damaging debris (D_{deb}) are defined here as having a characteristic length (diameter) 1 mm ≤ D_{deb} < 10 mm in size, LNT debris (L_{deb}) are 1 cm ≤ L_{deb} <10 cm in size, and trackable debris (T_{deb}) are ≥10 cm.

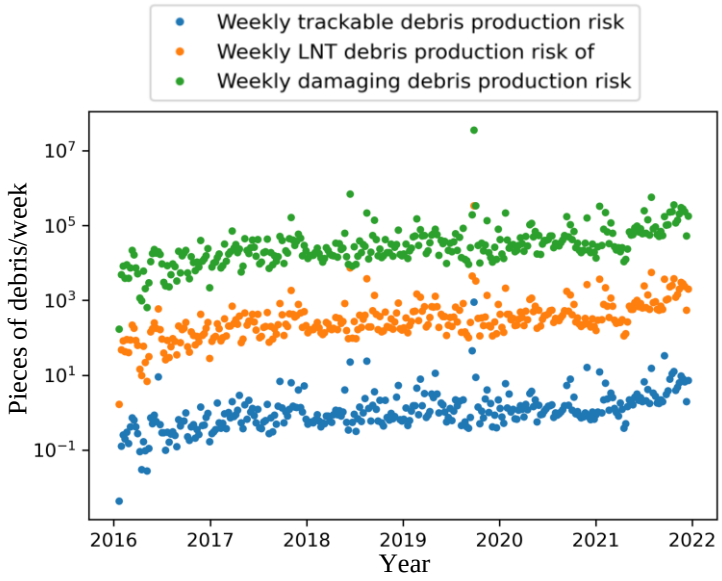

Fig. 7. Weekly total production of damaging (DMG), lethal non-trackable (LNT), and trackable (TRK) debris

Probably the most striking observation to make, other than the sheer scale of the number of damaging debris being predicted per week, is the fact that the risks appear to be slightly increasing, at a logarithmic rate. Each of the debris product bins follows a similar logarithmic distributions, with damaging and LNT being separated by two orders of magnitude, while the difference between LNT and TRK averages a difference of about 2.3 orders of magnitude. This was consistent for all results. Therefore, results for each debris category may not be shown from here forward. General trends for LNT and DMG debris can be extrapolated accordingly.

To validate whether the presence of a logorithmic increase is valid, a polynomial regression model was fit to the base 10 logarithm of the weekly total of TRK debris production risk. The data fit best with a third order model with each of the linear, quadratic, and cubic components being significant. Figure 8 shows the regression model of the total weekly risk, accounting for COLA maneuvers and the established Starlink vs. Starlink RRF of 169. Parameters for the COLA & Starlink RRF cubic model are as follows: R^2_{Adj} = .378, p_{value} < .001. Intercept = -0.91402, t = -9.78, linear: β = 0.01825, t = 7.00, p < .001; quadratic: β = -0.00011, t = -5.61, p < .001; cubic: β = 2.1846e-7, t = 5.28, p < .001).

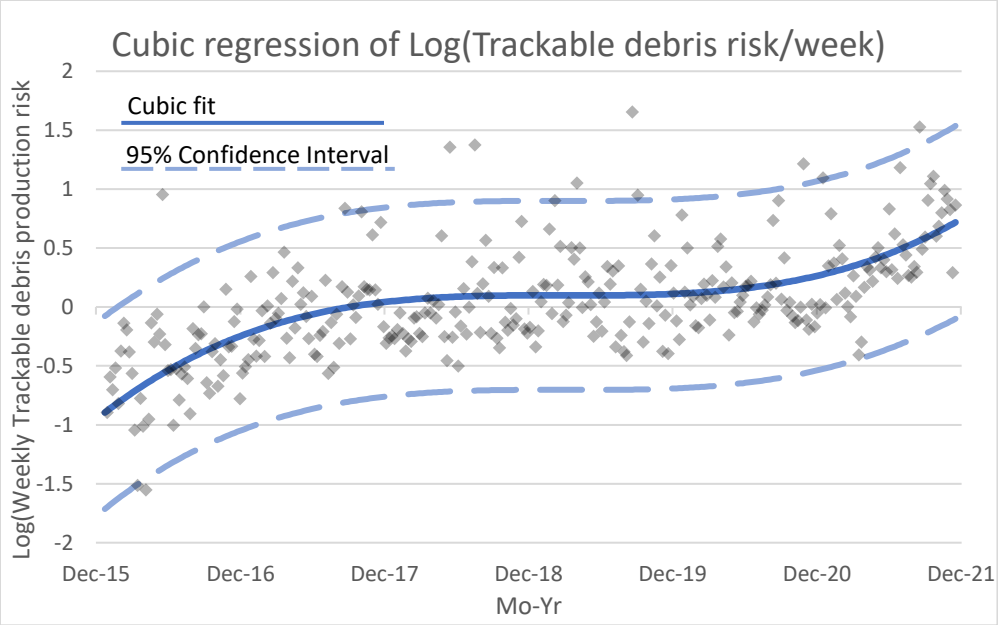

Fig. 8. Cubic fit of Log(weekly TRK debris production risk) with Starlink RRF & 95% confidence interval

The model indicates the rate of logarithmic increase may have been slowing prior to 2020. The significant linear component indicates a continual increase in risk over time. However, it appears from this analysis, that the rate of increase was slowing until about the 200th week (late 2019). Then the logarithm of the risk rate began to rise again, non-linearly. Follow-on annual analysis of these data is warranted to further evaluate the evolution of this trend in the future.

Another aspect of this distribution is the presence of several high-risk weeks. There were twelve occasions over the past six years of extremely high-risk events which had a risk of trackable debris production above six pieces of trackable debris each. These events dominated their respective week's total risk. These events are shown in Table 3. The vast majority of these events tended to have a mitigation factor of 1, i.e. they were not mitigatable. They were also all relatively large objects with probabilities of collision of >0.1%.

Table 3. Highest risk events for debris production between 2016 and 2021

Rank #	Date	SAT1_NAME	SAT2_NAME	MISS_DISTANCE (m)	Recomputed F-92	TRK_RISK (pieces)
1	18-Sep-19	GENESIS 2	COSMOS 1300	8	0.4655	897
2	6-Sep-19	YAOGAN 6	THOR AGENA B DEB	46	0.0467	45
3	6-Sep-21	SPACEBEENZ-10	COSMOS 1703	27	0.0272	32
4	9-Aug-18	HAIYANG 1B	IRIDIUM 33 DEB	10	0.0694	23
5	3-Jun-18	CICERO 7	COSMOS 546	12	0.0467	22
6	18-Nov-20	COSMOS 2455	NOAA 16 DEB	83	0.0057	15
7	1-Jan-21	ENVISAT	UNKNOWN	98	0.0025	10
8	24-Apr-19	TIANWANG 1B	ISS (ZARYA)	49	0.0054	10
9	9-Jun-16	BEAKERSAT 1	COSMOS 1743	47	0.0109	9
10	21-Jul-21	METEOR-M	UNKNOWN	82	0.0046	8
11	22-Sep-19	YAOGAN 7	YAOGAN 4	59	0.0019	8
12	26-Feb-19	TERRA	METEOR 2-9 DEB	90	0.0030	7

Figure 9 identifies these events as they occur in time along with the weekly risk. There is a near 1:1 correlation between the list of events in Table 3 and the rank order of the top 12 weeks' total risk. This indicates such events are

rare and explains that these events are responsible for driving the week's total risk. Taken together, these twelve events alone represent about 70% of the total debris production risk, while the number one event in the dataset alone represents over half of the total risk incurred over the six-year span. This firmly reinforces others' findings that large derelict objects are the highest priority candidates for debris remediation efforts [26]. The keen-eyed reader may notice that assumption (l) breaks down for at least one of the events listed in Table 3, #8 on the list involves the International Space Station (ISS), which is in fact maneuverable, and with a Pc above 1e-4 one would expect it would have been mitigated. However, due to the criteria applied to assumption (l) coupled with the fact that the ISS maintains the international designator of the it's first module (Zarya, ID:1998-067A), the object was assumed to be non-maneuverable, though in reality, it is maneuverable. This limitation will be addressed in future work. Though, each other conjunction on this list involved non-maneuverable objects such as rocket bodies and large debris larger than one square meter. If given different thresholds for assumption (l), the list of events changes, however the commonality that the list of highest risk events is predominantly represented by events which are non-mitigatable is a constant. Unfortunately, many of these such events are not captured in CDM reports due to differences in screening criteria for events which do not involve a payload object.

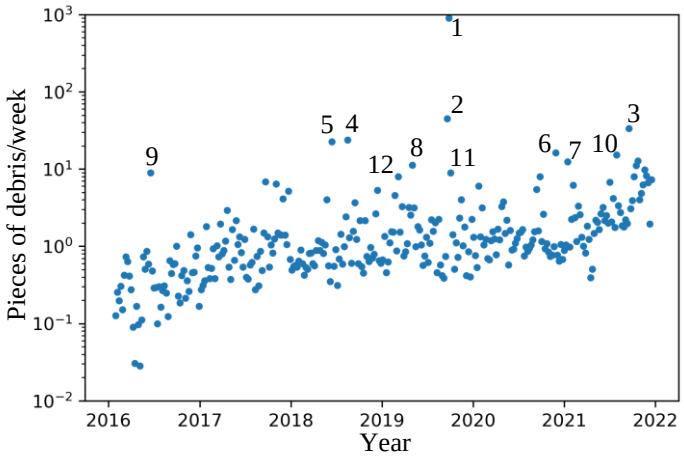

Fig. 9. Weekly risk of TRK production shows top 12 weeks correlate in time with top 12 events

4.2 Risk analysis by object type

After accounting for the Starlink RRF the remaining risk was broken out by the three largest LEO communications constellations, Iridium, OneWeb, and Starlink. Figure 10 shows the total risk of damaging debris. It is not driven by any one constellation for most weeks, though the combination of remaining Starlink and OneWeb risks constitute a significant portion of the risk for several weeks starting in 2020 and beyond.

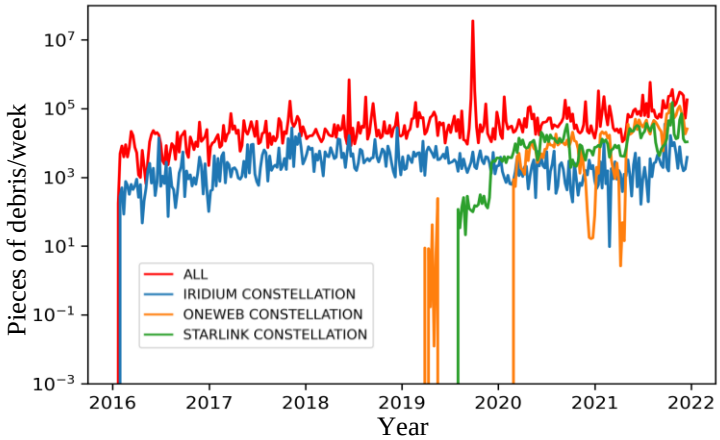

Fig. 10. Remaining weekly constellation risk of damaging debris creation, with COLA & Starlink RRF

However, the presence of white space between each of the constellations and the total risk line indicates that while large satellite constellations are creating an upward pressure on the risk baseline, conjunction events involving objects not associated with large constellations are also a significant contributor to the total risk per week. This is consistent with the findings from Table 3. An analysis of the breakdown of risk over time for different object types in the catalog is useful to validate this. Figure 11 shows the breakdown between large debris, payloads, rocket bodies, and small debris, for damaging debris.

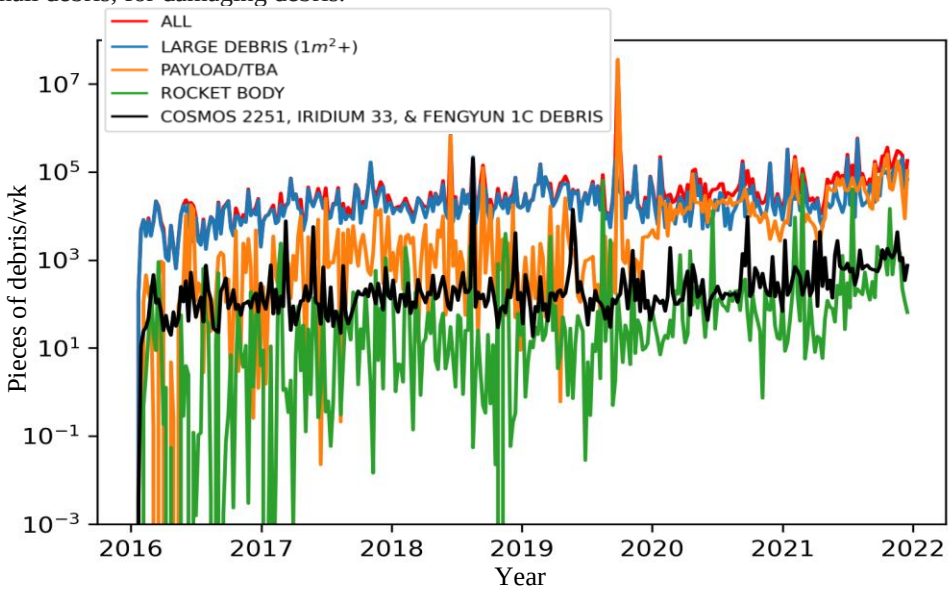

Fig. 11. Weekly object type risk of producing 1-10 mm debris (accounting for COLA & Starlink RRF)

Similar to the findings from Table 3, large debris objects have been primary contributors to the total risk each week. Though, during and after 2020, the largest risk contributor to payloads has become other payloads for some weeks. Rocket bodies appear to pose about two orders of magnitude lower risk in terms of expected debris production. This is not to say that Rocket Bodies are not hazardous. In fact, according to the data from the IMPACT test runs, the consequences of Rocket Body collisions tend to be extremely high [12]. However, in this dataset there are relatively few conjunction events involving Rocket Bodies. This is due to both the relatively low number of Rocket Bodies in the environment compared to payloads and large debris but is also likely due to rocket bodies and large debris not being screened as primary objects until Sept 2020, and then only reported when conjunctions reach emergency reportable criteria. This is consistent with assumption (e.). This analysis would benefit from having similar screening and reporting criteria for such objects and would offer a more complete dataset which may show different results for the total risk. Interestingly, the debris from COSMOS 2251, IRIDIUM 33, and FENGYUN 1-C combined constituted only about 1% of the total risk for debris generation. This stands to reason as such debris objects tend to be smaller. Nonetheless, these objects are lethal to operational vehicles, but the risk of knock-on debris generating events appears to be significantly lower than for their parent events.

4.3. Spatial domain risk analysis

Analyses over altitude show that there are risk spikes at 500 to 550 km, as well as at 800 km. (Figure 12). They also indicate that the risk of debris generation is substantially lower below an altitude of about 450 km, than above it.

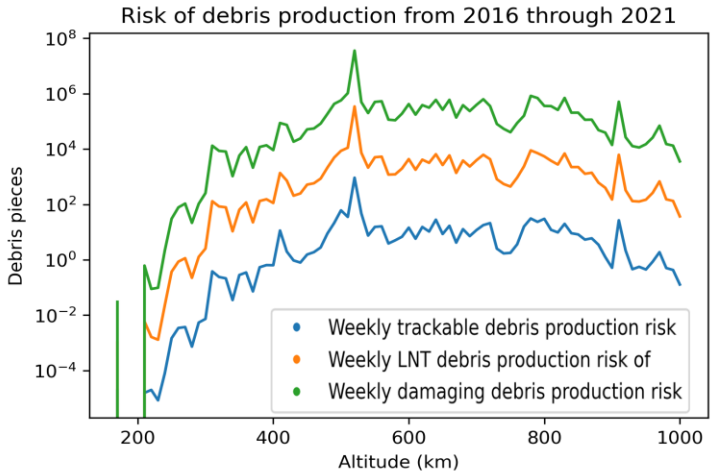

Fig. 12. Remaining production risk of DMG, LNT, & TRK debris by altitude

Figures 13-14 integrate both the spatial and temporal data to yield a heatmap which indicates the severity of risk over time by one-week bins and by altitude by 10 km bins. There is a clear pattern prior to 2020 at the altitude of Iridium, as well as other common altitude ranges between 500 to 700 km. In 2020 launches of both Starlink and OneWeb appear to have significantly affected the historical risk rate. By the end of 2021, most altitudes showed an increase in risk, especially when OneWeb launches and ascends through the different altitude regimes which is clearly visible as the diagonal streaks which increase with altitude over time. When OneWeb is not ascending, the background risk appears to remain somewhat static. Additionally, there are horizontal bands of risk which appear at around 550 km, 400 km, 370 km, and 340 km, which roughly correspond to Starlink's operational and early orbit checkout altitudes, respectively.

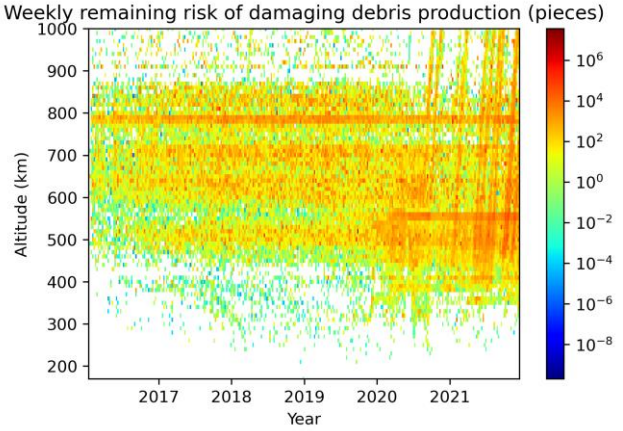

Fig. 13. Time/Altitude risk of DMG debris creation

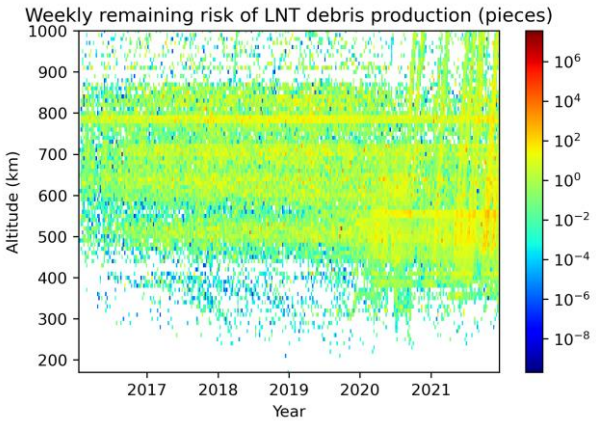

Fig. 14. Time/Altitude risk of LNT debris creation

For scale reference, a log plot and linear plot are provided in Figure 15 and 16 respectively. There is a stark difference between the visualization of the risk between the two figures. Figure 15 shows a log scale similar to Figure 13 and 14, while Figure 18 shows a linear scale with a different color scale. Figure 16 shows the same information as Figure 15, but the color is re-scaled linearly, to show high risk events which are indicated by the circles. All events with debris production risk higher than 10 trackable pieces were set to the color white. Otherwise, there would be only one white mark. The 12 events taken from Table 3 and circled in Figure 16 account for about 70% of the total debris production risk. This supports the position that while the background risk of collisions after accounting for COLA and Starlink RRF is increasing due to the presence of large constellations, the preponderance of the total collision risk resides with a small number of high-risk events which involve objects which likely cannot perform COLA maneuvers.

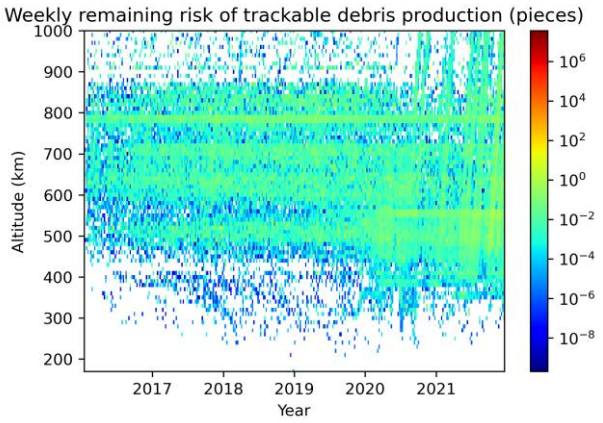

Fig. 15. Log(Time/Altitude risk of TRK debris creation)

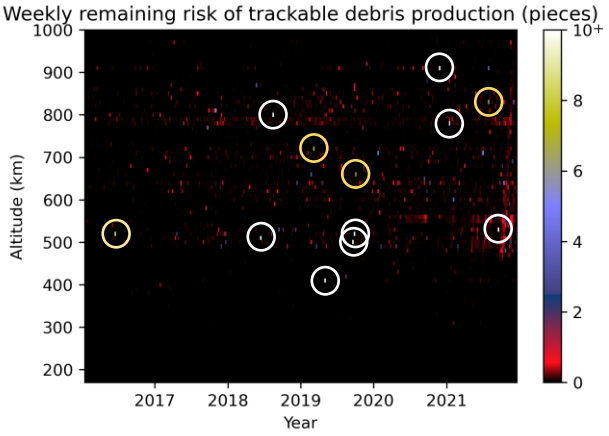

Fig. 16. Time/Altitude risk of TRK debris creation (re-scaled to show high-risk events in white & yellow)

Lastly, Figures 17 and 18 show the average annual risk of LNT debris generation by latitude and longitude, using a 2x2 degree grid. Figure 17 shows that the geographical distribution of risk between 2016 and 2019 was largely randomly distributed with concentration towards the poles (keeping in mind Mercator projections at extreme latitudes exaggerate spacing making the density appear artificially low). Figure 18 shows the geographical distribution of risks between 2020 and the end of 2021. A very different pattern emerged. Most notable is the band of risk which appears at ±50 degrees latitude. A higher density of near-polar risk is also apparent. The higher background risk which has emerged in the last few years is currently largely localized to both the altitude and peak latitude bands of the large communications constellations, likely because the spacing between self vs. self conjunctions is lowest at extreme latitudes, which can reasonably be expected to correspond to higher Pc and higher risk. Though again, the overall risk is clearly dominated by individual events which drive the risk for a given altitude/longitude (shown as dark red).

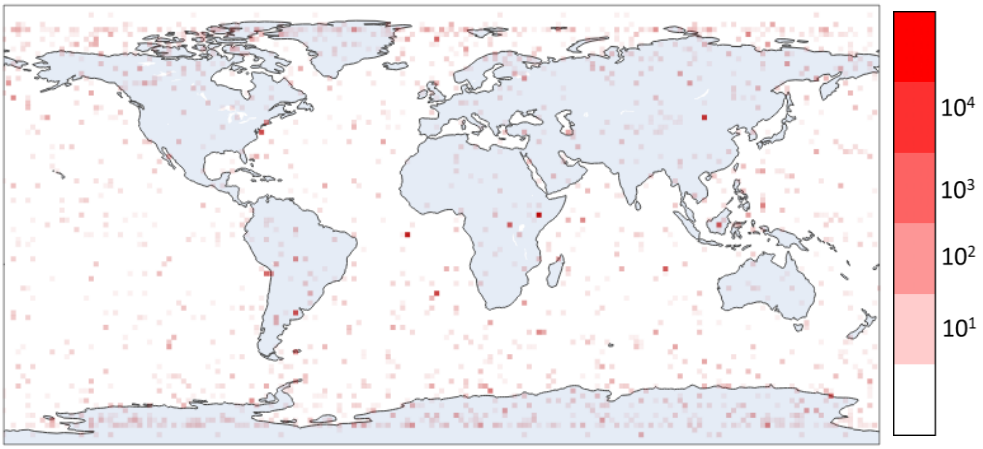

Fig. 17. Annual LNT production risk by Latitude/Longitude, from 2016-2019

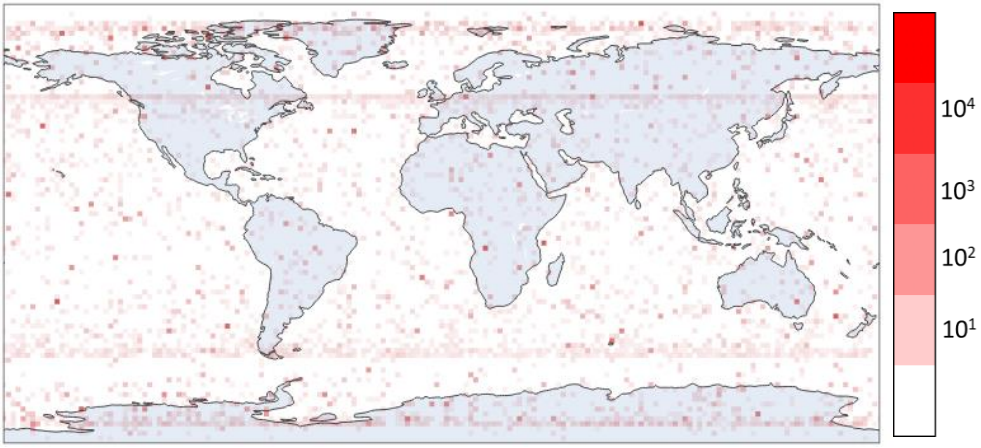

Fig. 18. Annual LNT production risk by Latitude/Longitude, from 2020 & 2021

5. ANALYSIS SUMMARY

This analysis saw an evolution of risk understanding by accounting for expected COLA maneuvers and treatment of self vs. self risk reduction. Integrated risk metrics for damaging, LNT, and TRK debris are provided below, first without considering COLA mitigation, then with, and finally, accounting for the Starlink RRF. After accounting for COLA and the Starlink RRF, approximately 10% of the risk remained. This may be useful as a value metric for how much performing the CA mission improves the outlook for environmental sustainability in the short to intermediate-term.

Total risk without COLA mitigation
- DMG (1 mm - 1 cm) = 684,284,039 pieces of debris (114,047,340/yr)
- LNT (1 cm - 10 cm) = 7,076,452 pieces of debris (1,179,409/yr)
- TRK (10 cm +) = 21,547 pieces of debris (3,591/yr)

Total risk with COLA mitigation (if payloads <10yrs old, >100 kg, & re-computed Pc > 1e-4; set Pc=1e-6)
- DMG (1 mm - 1 cm) = 55,971,107 pieces of debris (9,328,518/yr)
- LNT (1cm-10 cm) = 562,422 pieces of debris (93,737/yr)
- TRK (10 cm +) = 1,722 pieces of debris (287/yr)

Total risk with COLA & Starlink RRF
- DMG (1 mm - 1 cm) = 50,892,824 pieces of debris (8,482,137/yr)
- LNT (1 cm - 10 cm) = 511,163 pieces of debris (85,194/yr)
- TRK (10 cm +) = 1,576 pieces of debris (263/yr)

1,200 pieces of these expected 1,576 TRK pieces originated from only the top fifty conjunction events, constituting over 75% of the debris generation risk but only 0.01% of the conjunction events over the six years studied.

With a top level metric of 1,576 TRK pieces the research team sought to compare this values to what has been historically observed. To bound these results to historical observations, a query for all OBJECT_TYPE = Debris, with SATNO >41238 and < 50803 was generated from space-track.org. This range was determined by searching for the first piece cataloged from a launch in 2016 (SATNO 41238), and the first object cataloged from a launch in 2022 (SATNO 50803). The query returned the following:

- 4,337 tracked pieces of debris were cataloged between 2016 and the end of 2021.
- 3,591 of those had a perigee of <1,000 km
- 1,142 of the remaining 3,591 were related to rocket body breakups
- This left 2,449 pieces emanating from vehicle payloads/satellites. Of the payload-related debris pieces:
    - 1,004 were related to COSMOS 1408 ASAT test
    - 129 were related to the Indian ASAT test
    - 106 were related to the Fengyun 1C ASAT test
    - This leaves approximately 1,200 pieces of cataloged debris from non-ASAT events

However, after accounting for other confirmed and probable failure modes, from the list of objects each piece of debris was associated to, no more than 19% (700 pieces) likely emanated from breakup events with unknown or unconfirmed, failure modes, which may be collision candidates. There was one confirmed payload collision between two trackable objects between 2016 and 2021. This accounts for no fewer than 37 pieces of cataloged debris. This occurred on 18 March 2021 when Yunhai 1-02 and a piece of debris from a Russian Zenit-2 launch vehicle collided [27]. 37 pieces of debris (6/yr) serves as an observed lower bound for the debris population, commensurate with the CDM data analyzed for the period. NASA has studied the proportion of cataloged satellite breakup debris remaining in orbit and has published the illustration shown in Figure 21 [28]. It shows that 14.3% (514 pieces) of debris in orbit may emanate from accidental collisions. Using this estimate as an upper bound places the debris generation rate between 6 and 85 pieces of cataloged debris per year. However, this likely includes some cataloged payload debris generated by collisions with uncataloged objects, which is outside the set of events captured by CDMs.

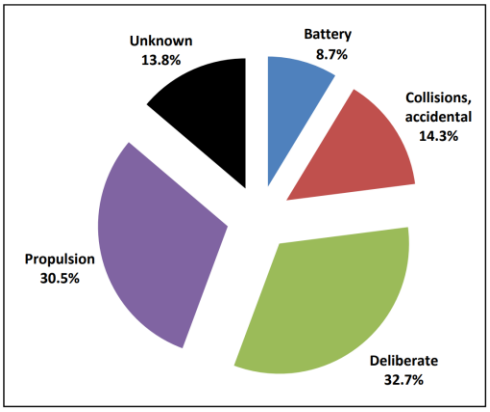

Fig. 21. Proportion of cataloged satellite breakup debris remaining in orbit [28].

This indicates that the computed debris production rate from this work may be between 2 to 40 times the production rate otherwise expected, though with a single confirmed event, it is impossible to provide a confidence interval to bound the feasibility of this finding. To address this, a historical search of all four instances of confirmed tracked debris collisions between a satellite and another cataloged object yielded a mean of 77.81 pieces per year with a very wide bootstrapped 95% confidence interval of between 0.01 and 230.7 trackable pieces of debris generated per year from collisions between payloads and other trackable objects. This is slightly less than the 263 trackable pieces per year estimated in this work and is within a half-order of magnitude of other estimates. Given this research has known residual conservative bias with the assumptions and limitations discussed (f.), and (g.). This leaves room for methodological improvements to bound the production rate more accurately. Doing so may allow for the development of a metric for LNT and DMG debris production which is linked to validated semi-empirical models and empirical observations of historical events, which has been demonstrated here for the first time. Clearly, further study along this front of research is warranted for use in the areas of operations research and space policy development.

6. FUTURE WORK

Regrettably, ESA DISCOS mass and data for objects in the catalog were not integrated with this analysis, but future analyses will include DISCOS data. Future work also seeks to take advantage of Hall's 3D Pc computation, which is expected to yield more reliable Pc estimates [29]. Partial mass interactions due to glancing blows will also be accounted for by considering a mass interaction ratio of 50% when the two objects' radii have a ratio of <2. When the radii ratio is >2, full mass interaction will be assumed. Additionally, refinements can be made for selection of which CDM should be used for analysis for each event by accounting for the most robust CDM in the last two days prior to TCA which was also expected to be the final CDM prior to any mitigating action.

Looking further out, future researchers could make use of the velocity distributions for debris objects present in the IMPACT 8.0 results to estimate orbital lifetimes of debris products based on the state vectors, approach vectors, assumed mass interaction ratios, and mass distributions of the colliding objects. Doing so would better inform the temporal component of the risk of daughter collision debris particles. This would in-turn help inform more useful figures of merit for policy makers and better inform the time variant risk to the sustainability of the LEO environment from collisions, as well as from knock-on collision events. Future work also seeks to expand the

analyses to include higher altitudes and extend into other orbital regimes. Upcoming analyses will also investigate a list of highest risk objects and compare these results with previously published studies of a similar nature, though a more complete assessment of maneuverability status and more uniform sampling of conjunction events which do not involve payloads is necessary to make comparisons with [26]. An avenue to accomplish this is to develop a wider cross-reference by common names of satellites such as NOAA and DMSP for example, which are known to be <10 years old and >100 kg threshold be non-maneuverable.

7. CONCLUSIONS

This work is the first effort to quantitatively analyze and integrate historical risks of conjunction events from empirical data and fuse them with the latest semi-analytical breakup algorithms to reveal the distribution and evolution of collision risks in LEO. This work has demonstrated a method to accomplish that, and the results show changes in how humanity is accessing and utilizing space has increased the risk of collisions at all orbital altitudes below 1,000 km. While the integrated risk values themselves stand to be improved to match reality more closely, there is a path to achieve that goal. However, regardless of any possible bias in the data, the trends are clearly increasing over time and more work needs to be done to better quantify the consequences of these risks through the time domain. One of the more important applications of these data may be to inform policy decision makers about the existing risks and how they're changing to better inform the questions of how severe the problem of orbital debris is, and what should be done about it. had a predicted risk of debris production greater than ten trackable pieces and occurred between defunct satellites and large debris which could not be mitigated. If they had been, this would have removed over two thirds of the total risk of debris generation over the span of the six years of conjunction events analyzed. This indicates that improvements to screening criteria for rocket bodies and all objects above one square meter would offer a more complete risk assessment. These findings also indicate that updated space safety policy may have a large and lasting beneficial impact to the environment. Such policies include debris mitigation guidelines, minimum maneuverability guidelines, post-mission disposal reliability rates, and other end-of-life operational requirements. These results also indicate that emerging debris removal efforts stand to make the largest gains in risk remediation by focusing on large, defunct objects which have surpassed the end of their usefulness. Further analyses of these data are expected to be valuable for generating estimates and metrics to trend collision risks and risks to the LEO environment's sustainability over time, using a large set of empirical CDMs with current semi-analytical breakup models. This is the first known attempt to demonstrate this capability which is useful towards achieving gains in the fields of space systems design safety, operations, operations research. These analyses can also inform ongoing and future space policy development efforts at departmental, national, and international levels.

8. DISCLAIMER

The views and opinions expressed or implied are those of the authors and should not be construed as carrying the official sanction of the Department of Defense, Department of the Air Force, Air Education and Training Command, Air University, or other agencies or departments of the US government.

9. REFERENCES

[1] Air Force Instruction 91-202. (2020, Mar. 12). *The US Air Force Mishap Prevention Program.* paragraph 1.6.10.20. https://static.e-publishing.af.mil/production/1/af_se/publication/afi91-202/afi91-202.pdf.

[2] Moomey, D., Potter, A., Matchett, J. C., & Thielke, J. (2020). Trending analysis of historical conjunction data messages. *Journal of Space Safety Engineering*, 7(1), 44–51. https://doi.org/10.1016/j.jsse.2019.12.003

[3] Thompson, R., Jenkin, A., Sorge, M., Peterson, G., Mcvey, J., Yoo, B., Hansen, B., Starchville, T., & Hoots, F. (2015). *Crosslink® The Aerospace Corporation magazine of advances in aerospace technology Understanding Space Debris Causes, Mitigations, and Issues*. https://aerospace.org/paper/crosslink-fall-2015

[4] NASA, NASA Spacecraft Conjunction Assessment and Collision Avoidance Best Practices Handbook. Washington DC, 2020. https://nodis3.gsfc.nasa.gov/OCE_docs/OCE_50.pdf

[5] Balch, M., Martin, R., Ferson, S., (2019). Satellite conjunction analysis and the false confidence theorem. *Proc. R. Soc. A* 475: 20180565. http://dx.doi.org/10.1098/rspa.2018.0565

[6] Elkantassi, S., Davison, A. C., Space Oddity? A Statistical Formulation of Conjunction. (2021). *Stat.AP.*, https://arxiv.org/pdf/2106.09541.pdf

[7] Hedjuk, M.D., Snow, D.E., Newman, L.K., (2019). Satellite Conjunction Assessment Risk Analysis for "Dilution Region" events: Issues and Operational Approaches. NASA, NTRS. https://ntrs.nasa.gov/api/citations/20220004539/downloads/Hejduk%20and%20Snow%202019.pdf?attachment=true
[8] 18th Space Control Squadron (Vandenberg Air Force Base, CA, USA). *Spaceflight Safety Handbook for Satellite Operators*. (2020). (accessed Aug. 31, 2020). https://www.space-track.org/documents/Spaceflight_Safety_Handbook_for_Operators.pdf
[9] 18th Space Control Squadron Mission Brief (accessed 22 September 2020). http://mstl.atl.calpoly.edu/~workshop/archive/2017/Spring/Day%202%20/Session%201/1a_18SPCS.pdf
[10] The Consultative Committee for Space Data Systems (Washington, DC, USA). *Conjunction Data Message Recommended Standard CCSDS 508.0-B-1* Blue Book (2013). https://public.ccsds.org/Pubs/508x0b1e2s.pdf
[11] SAIC, under contract to CFSCC CJ3/6. Space-Track.org. https://www.space-track.org. (accessed, 29 Aug 2022).
[12] Moomey, D., Falcon, R. Cox, K., Sorge, M., "Development of a historical conjunction data message database for space sustainability trending and analysis" 3rd IAA Conference on Space Situational Awareness, Madrid, Spain, April 4-6, 2022.
[13] M. Horstman, V. Papanyan, Q. Juarez, and J. Hamilton, "Haystack ultra-wideband satellite imaging radar measurements of the orbital debris environment: 2014-2017," NASA Orbital Debris Program Office, Tech.Rep. NASA/TP-2014-217391, 2014. https://ntrs.nasa.gov/api/citations/20190028719/downloads/20190028719.pdf
[14] Ghio, S., Martorella, M., (2020). Size estimation of space debris models from their RCS measured in anechoic chamber. Proceedings from the 17th European Radar Conference. https://ieeexplore.ieee.org/document/9337465
[15] Union of Concerned Scientists. UCS Satellite Database. https://www.ucsusa.org/resources/satellite-database. (accessed, 29 Aug 2022).
[16] Krebs, Gunter D. *"Gunter's Space Page"*. Gunter's Space Page. https://space.skyrocket.de/index.html. (accessed 29 Aug 2022).
[17] Scikit-learn: Machine Learning in Python, Pedregosa *et al.*, JMLR 12, pp. 2825-2830, 2011.
[18] Astrorum Inc. Omitron Inc., (2021). Software Development Kit: Software Development Kit: Two-Dimension Probability of Collision (Pc) Calculations. NASA GSFC.
[19] D.L.Mains, M.E.Sorge, "Integrated breakup modeling solutions from DebriSat analysis", The Aerospace Corp., presented at the First Int'l. Orbital Debris Conf. (2019). no.6025.
[20] P.M. Sheaffer, P.M. Adams, N. Hemmi, C. Hartney, "DebrisLV Hypervelocity Impact Post-Shot Physical Results Summary", Aerospace Report No. TOR-2014-03577, Feb 27, 2015.
[21] D.L. Mains, M.E. Sorge, "The IMPACT Satellite Fragmentation Model", The Aerospace Corp., presented at the 72nd IAC, Dubai, UAE, Oct. 25-29, 2021. IAC-21-A6.2.1.
[22] SpaceX corp., presentation in conference, SSA operator's workshop (Boulder, CO, USA, May 31 – Jun 3, 2022)
[23] Network Access Associates Ltd., presentation in conference, SSA operator's workshop (Boulder, CO, USA, May 31 – Jun 3, 2022)
[24] Iridium Communications Inc., presentation in conference, SSA operator's workshop (Boulder, CO, USA, May 31 – Jun 3, 2022)
[25] SpaceX Corp., SpaceX Updates. (accessed, 12 Aug 2022). https://www.spacex.com/updates/
[26] McKnight, D., Witner, R., Letizia, F, et.al., (2021). Identifying the 50 statistically-most-concerning derelict objects in LEO. *Acta Astronautica*, *181*, 282–291. https://doi.org/10.1016/j.actaastro.2021.01.021
[27] Jones, A.. "Breakup of China's Yunhai-1 (02) satellite linked to space debris collision." Space News. https://spacenews.com/breakup-of-chinas-yunhai-1-02-satellite-linked-to-space-debris-collision/ (retrieved May 16 2022).
[28] Anz-Meador P.D. "Debris by the numbers" A précis of the NASA History of On-orbit Satellite Fragmentations, 15th Ed.. NASA ODPO. *Orbital Debris Quarterly News*, V.23, Issue 1&2, p.7. May 2019. https://orbitaldebris.jsc.nasa.gov/quarterly-news/pdfs/odqnv23i1.pdf
[29] Hall, D. (2021). Software Development Kit: Three-Dimensional Probability of Collision (Pc) Calculations. NASA GSFC. https://github.com/nasa/CARA_Analysis_Tools/tree/master/ThreeDimensionalPc/Documentation